



## Short-term culture of monocytes as an *in vitro* evaluation system for bionanomaterials designated for medical use



Ekaterina Igorevna Shishatskaya<sup>a</sup>, Dragana Nikitovic<sup>b, \*\*</sup>,  
Alexander Shabanov Vasilievich<sup>c</sup>, George N. Tzanakakis<sup>b</sup>, Aristidis M. Tsatsakis<sup>d, \*</sup>,  
Natalia Gennadievna Menzianova<sup>a</sup>

<sup>a</sup> Siberian Federal University, Svobodnuy Av. 79, Krasnoyarsk, 660041, Russia

<sup>b</sup> Laboratory of Anatomy, Histology, Embryology, School of Medicine, University of Crete, Heraklion, 71003, Greece

<sup>c</sup> Institute of Physics, Russian Academy of Science, Siberian Division, Akademgorodok, 50, Build. 38, Krasnoyarsk, 660036, Russia

<sup>d</sup> Laboratory of Toxicology, Medical School, University of Crete, Heraklion, 71003, Greece

### ARTICLE INFO

#### Article history:

Received 29 June 2016

Received in revised form

18 August 2016

Accepted 19 August 2016

Available online 21 August 2016

#### Keywords:

Biocompatible biopolymers

Polyhydroxyalkanoates

Nanomaterials

Nanodiamonds

Fullerenes

Bio-nanomaterials

Monocytes

### ABSTRACT

We studied the feasibility of using a short-term culture of monocytes, isolated from peripheral donor blood, to assess the biological activity of different types of bionanomaterials (BNM): biodegradable polymeric particles, fiber and film substrates of micro- and nano-dimensions, fullerenes (F) and nano-diamonds (ND), which are either currently in use and/or potentially applicable in medicine. Additionally, the effect of creating a protein corona on ND and F particles was investigated. The cellular reduction of (4,5-dimethylthiazol-2-yl)-2,5-diphenyltetrazolium bromide (MTT) is a well-established tool for assessing the viability/metabolic activity of cells. The scanning electron microscopy assay can detect fine changes in cell morphology. In the present study BNM have been shown to affect; in a size, chemical composition and morphological characteristics-dependent manner, the ability of monocytes to reduce MTT as well as their morphology. Moreover, the specific effects of ND and F on MTT reduction and cell morphology were exhibited in a dose-dependent manner and sensitive to the formation of surface protein corona. Our results suggest that short-term culture of monocytes is a sensitive model system for assessing the biological effects of BMPs *in vitro*.

© 2016 Elsevier Ltd. All rights reserved.

### 1. Introduction

Nanoparticles (NPs) are characterized by their small size (1–100 nm in diameter), unique ratio of surface area to volume, multiple variations in particle shape, as well as discrete mechanical, optical, magnetic and electronic properties (Farokhzad and Langer, 2006; Kuskov et al., 2010). The widespread use of nanomaterials in regenerative technologies, diagnostics and targeted therapy (Piperigkou et al., 2016) is complicated by their cytotoxic side effects (Khalili et al., 2015; Shishatskaya et al., 2012). An important facet of nanomaterial toxicity, and due to their structural properties, is the induction of mechano-chemical signal translation.

Thus, the interactions of nanomaterials with biomembranes,

through the application of different physical forces change cell morphology and may lead to the activation of an unique receptor-independent signaling mechanisms which translate membrane deformations into chemical signal transduction cascades (Galic et al., 2014; Echarri and Del Pozo, 2015). Therefore, these physical forces, arising in the plasma membrane during the interaction and the internalization processes of the NPs, trigger nanoscale membrane deformations, which are then translated into biochemical signals regulating various biological functions (Bharde et al., 2013; Lee et al., 2014; Curtis and Tsimbouri, 2014; Henstock et al., 2014; Henstock and Haj, 2015; Kilinc et al., 2016). Indeed, ambiguous effects of NPs on cell differentiation and proliferation as well as on lipid metabolism can also be linked with non-receptor signaling cascades (Klotzsch et al., 2015).

The biological effects of NPs, including their cytotoxicity, can be largely modified with the formation of protein “corona”, formed through adsorption of various proteins on the surface of the NPs. Features of protein corona (PC), determine the manner of

\* Corresponding author.

\*\* Corresponding author.

E-mail addresses: [nikitovic@uoc.gr](mailto:nikitovic@uoc.gr) (D. Nikitovic), [aris@med.uoc.gr](mailto:aris@med.uoc.gr), [tsatsaka@uoc.gr](mailto:tsatsaka@uoc.gr) (A.M. Tsatsakis).

internalization, the cascades of intracellular signaling and effector targets, including lipid metabolism system, redox homeostasis, proinflammatory and anti-inflammatory responses (Fleischer and Payne, 2014; Mortimer et al., 2014; Hata et al., 2014; Shannahan et al., 2015; Matczuk et al., 2015; Di Silvio et al., 2015; Zanganeh et al., 2016; Polyak and Cordovez, 2016).

Cytotoxicity, non-receptor signaling as well as the formation of the PC underlie the ambiguity of NPs effects and reduce their effectiveness as therapeutic agents and bioimplants (Neagu et al., 2016). Therefore, the establishment of effective evaluation systems for assessing NPs and bionanomaterials (BNMs) biological activity *in vitro* is mandatory. Suitable assays allow selection of the most “safe” version of nano-sized particles and materials as well as facilitate their use for functional engineering in medicine.

Short-term culture of monocytes, isolated from peripheral blood of healthy donors or patients, as a system for BNMs screening is one of the biologically “reasonable” options. This approach is further supported by the fact that the clearance of NPs and biodegradation of nanocomposite implants *in vivo* depend largely on the functional activity of the monocyte-macrophage system (Damanik et al., 2014; Trindade et al., 2014; Zandstra et al., 2014; Anderson, 2015; Majd et al., 2015). Moreover, a simple well-reproducible procedure for the separation of monocytes from peripheral blood enables the establishment of a high through output evaluation system, capable of assessing the individual features of the BNMs biological effects. This is all the more important as the functional monocyte-macrophage activity *in vitro* (for example, the ratio of phenotypes M1 and M2) varies considerably among different donors (Damanik et al., 2014; Grotenhuis et al., 2014).

Typically in *in vitro* screening systems the effects of the tested factors on specific integral parameters, e.g. cell viability and morphology are evaluated. Analysis of integral parameters is sufficient to address the specific interim goals and select the most promising groups of BNMs for further functionalization and application in medicine. Therefore, we investigated the feasibility of using monocyte short-term culture for *in vitro* evaluation of different BNMs effects, utilizing changes in metabolic activity and cell morphology as end points.

## 2. Materials and methods

### 2.1. Materials

Biopolymer BNMs - particles, fibers and film substrates - were prepared from the group of polyhydroxyalcanoates (PHAs) biopolymers, synthesized in culture *Ralstonia eutropha* B5786 in specific cultivation conditions. The polymer samples were provided by the head of Laboratory of Chemoautotrophic biosynthesis of Institute of biophysics, RASSD, professor, Dr. Tatiana Volova. As reference representatives of polymer biomaterials from the same chemical group, and widely in use in medicine as implantable materials polylactic acid, PLA, and polylactic-co-polyglycolic acid, PLA/PGA (Sigma, USA) were used. Stable aqueous suspensions of nanodiamonds (ND) and fullerenes (F) were provided by Alexey Puzir, Laboratory of Biotechnology and Bioluminescence of the same Institute of Biophysics. The average diameter of ND was  $54,07 \pm 0,35$  nm, the polydispersity index  $PdI = 0,225 \pm 0005$ . The average diameter of F was  $94,64 \pm 3,12$  nm, polydispersity index  $PdI = 0,482 \pm 0031$ . Dimensional characteristics of ND and F have allowed us to imagine non-receptor internalization for these particles and the expected specific morphological changes of cell membranes.

### 2.2. Preparation of biopolymer particles, fibers and film substrates

The biopolymer particles and fibers substrates were prepared from poly-3-hydroxybutyrate (P3HB) and poly-[3-hydroxybutyrate-co-4-hydroxybutyrate] with 10 mol. % of 4-hydroxybutyrate inclusion (P3HB/4HB10). Films substrates were prepared from P3HB/4HB10. Biopolymer particles were prepared by evaporation of the solvent from the emulsion of viscous solutions of polymers. Shortly, the polymer solution in dichloromethane with 1% surfactant by adding 1% of polyvinyl alcohol was dispersed with a mechanical stirrer, fitted with a three-blade propeller and/or by « Sonicator » ultrasonic generator 3000 (Misonix Incorporated, USA). After evaporation of the solvent, microspheres were collected by centrifugation at 10 000 rpm/min, washed, dried under vacuum and lyophilized with Martin Christ ALPHA 2–4 LDplus (Martin Christ Gefriertrocknungsanlagen GmbH, Germany). The dimensions of particles obtained ranged from 20 nm to 500 nm. To isolate the fraction up to 200 nm, particles were suspended in DMEM, supplemented with 10% fetal bovine serum (FBS) and antibiotics (streptomycin 100 µg/ml, penicillin 100 U/ml, Gibco, Invitrogen, USA), and filtered through a membrane filter Sartorius, Germany. This fraction of particles we considered as nanosized. Membrane filters were rinsed with DMEM medium to obtain coarse fraction (particles greater than 200 nm, microsized). Fibers were obtained by the electrostatic spinning with Nanon 01A, MECC, Japan. 5% biopolymers chloroformic solutions were fed at a rate of 5 mL/h in an electric field of 6–30 kV. As representative biopolymers we used P3HB, its mixture with PLA as 50/50, and with PLA/PGA - P3HB + PL + PG, as 50/25/25; for PHB oriented and non-oriented substrates were assessed. Fat-free glass slides as the accepting target were used for all samples. The polymeric films were prepared by pouring of the P3HB/4HB10-chloroformic solutions on glass fat-free surface followed by complete evaporation of solvent in the laminar box at stable temperature and air flow. The protein corona on ND and F nanoparticles was preformed as follows. In short, 100% FBS was added to aliquots of sterile aqueous solutions of ND or F (1:1 by volume) and incubated for 5 min. The modified ND and F were diluted with DMEM, and 10% FBS to the required concentrations.

### 2.3. Isolation and cultivation of monocytes

Monocytes were isolated from peripheral blood of healthy donors in the density gradient of urografin/Ficoll by utilizing the Recalde method (1984). Isolated monocytes were resuspended in DMEM, 10% FBS, which is in continuation referred throughout the text as culture media (CM). The cells were allowed to attach during 2 h whereupon the non-adherent cells were removed by aspiration.

In experiments with P3HB- and P3HB/4HB10 – fiber substrates, the sterile substrates were placed on the bottom of 96-well culture plates, to which  $10^5$  cells in 160 µL CM per well were added. The thickness of film scaffolds was  $115 \pm 16$  µm, with an average diameter of 6 mm, well in correlation to the diameter the 96-well plate. In experiments with P3HB- and P3HB/4HB10 -particles  $10^5$  cells in 80 µL CM and 80 µL of particles solutions in CM per each well were added; the final particle concentration was 0,5 mg/mL. As a control, plates containing only  $10^5$  cells in 160 µL CM per well cultured on plastic were utilized. In experiments with ND and F sterile PHB-film substrates were placed at the bottom of the 96-wells for both control and treatment samples. For control samples  $10^5$  cells in 160 µL CM per well were added. In treatment samples  $10^5$  cells in 80 µL of CM and 80 µL of solution of NA or F in CM per well were added. The final F and ND - concentrations were 2,5 µg/mL, 25 µg/mL and 50 µg/mL, respectively. Both control and treated cells were cultured during 36 h in a CO<sup>2</sup> -incubator Sanyo, Japan.

**Table 1**  
The effects of biopolymeric particles/fibers on the ability of monocytes to reduce MTT.

Biopolymeric particles		Biopolymeric fibers	
Type of particles	MTT- assay, % of control treatment	Type of fibers	MTT- assay, % of control treatment
P3HB, < 200 nm	64 ± 7 <sup>^</sup>	P3HB, oriented fibers	80 ± 9
P3HB, > 200 nm	50 ± 7 <sup>^</sup>	P3HB, nonoriented fibers	59 ± 7 <sup>^</sup>
P3HB/4HB10 < 200 nm	64 ± 8 <sup>^</sup>	P3HB50 + PL25/PG25	75 ± 8
P3HB/4HB10 > 200 nm	95 ± 11 <sup>#</sup>	P3HB50 + PL50	77 ± 9

<sup>^</sup> – significant differences as compared to control treatment ( $p < 0.05$ ).

<sup>#</sup> – significant differences between P3HB/4HB10 > 200 nm and the P3HB/4HB10 < 200 nm treatments ( $p < 0.05$ ).

## 2.4. MTT-assay

The potential cytotoxicity of BNMs was evaluated by measuring the cellular reduction of MTT. Metabolic activity of cells was tested in all groups after 36 h. All tests were performed at least 3 times in order to ensure the reproducibility of results. Respectively, upon the completion of treatment, the test and control groups were exposed to sterile solution of 5 mg/ml MTT powder (Sigma Chemical Co, St Louis, MO, USA) in PBS, according to the manufacturer's instructions. All samples were then incubated at 37° C in humid atmosphere for another 4 h. Upon centrifugation of the plates the supernatant was discarded, cells were ruptured by addition of isopropanol and 0.04% hydrochloric acid (100 µl). The results were read by iMark™ Microplate Absorbance Reader (Bio-Rad, USA) at a wavelength of 570 nm considering 630 nm wavelength as the reference. The optical density (for  $\lambda = 570$  nm) of control samples was 100%. Readings of MTT-reduction in treated groups were expressed as a percentage of control.

## 2.5. Scanning electron microscopy assay

After completion of the incubation, the culture medium was removed and cells were fixed in plate wells with 2.5% glutaraldehyde (in phosphate buffer, pH = 7.4), for 1 h at 4° C. Post fixation of the samples was performed with 1% OsO<sub>4</sub> (in phosphate buffer, pH 7.4), 1 h at 4° C in refrigerator. The samples were washed twice with PBS, and dehydrated in ethanol ascending concentrations: 10%, 20%, 30%, 40%, 50%, 60%, 70%, 80%, 90% and 100% (twice), 5 min at each concentration at room temperature. After dehydration with ethanol, the scaffolds with adherent cells were removed from the wells and washed twice with 100% acetone. In continuation the scaffolds were attached to a copper plate and dried in vacuum-assisted desiccators overnight and then stored at room temperature till SEM analysis was carried out. The surface of the scaffolds was sputter-coated in a vacuum with an electrically conductive 5 nm thick layer of gold alloy Precession Etching Coating system

**Table 2**  
The effects of fullerenes (F) and nanodiamonds (ND) with and without a protein corona (PC) on the ability of monocytes to reduce MTT.

Treatment types	The concentration of nanoparticles in the culture medium MTT, %		
	2.5 µg/mL	25 µg/mL	50 µg/mL
<sup>b</sup> P3HB/4HB10 + F	94 ± 10 <sup>a</sup>	113 ± 16	100 ± 14
P3HB/4HB10 + (F + PC)	107 ± 10	116 ± 18	107 ± 12
P3HB/4HB10 + ND	104 ± 11	104 ± 13	143 ± 13 <sup>**</sup>
P3HB/4HB10 + (ND + PC)	107 ± 10	100 ± 8	88 ± 10

<sup>\*\*</sup> – significant differences among the control treatment (P3HB/4HB10 -biopolymer scaffolds) and the experimental models P3HB/4HB10 + (ND + PC), 50 µg/mL, ( $p < 0.05$ ).

<sup>a</sup> The results are expressed as MMT % of control.

<sup>b</sup> The thickness of film scaffolds was 115 ± 16 µm, with an average diameter of 6 mm, well in correlation to the diameter the 96-well plate.

(Gatan Model 682, Inc. USA). The prepared assay samples were analyzed by scanning microscope Quanta FEI 200 (USA) (Parameswaran and Verma, 2011). For each donor and treatment, 4–5 scaffolds with adherent cells were analyzed. On each scaffold 80–100 cells were counted in random fields and in continuation distributed according to morphological classes. The total number of analyzed cells was taken as 100%. The number of cells in different morphological classes is expressed as a percentage of the total number of cells.

## 2.6. Statistical analyses

Statistical analysis of the results was performed by conventional methods, using the standard software package of Microsoft Excel. Arithmetic means and standard deviations were found. Statistical significance was determined using Student's *t*-test. Statistically significant differences were accepted at  $P \leq 0.05$  level.

## 3. Results and discussion

### 3.1. Effects of P3HB- and P3HB/4HB10-biopolymeric particles and fibers on monocyte MTT-reduction

Optical density values as measure of cell viability had demonstrated marked variability among different treatments, depending on the chemical composition, structure and size of particles, as shown in Table 1. Thus, cultivation of cells in direct contact with P3HB/4HB10 particles larger than 200 nm (P3HB/4HB10, >200 nm) did not affect their viability as compared to control ( $P = NS$ ). On the other hand, exposure of cells to PH3B particles of the same size, >200 nm, caused a significant reduction in monocyte viability ( $p \leq 0.05$ ). The ability of monocytes to reduce MTT was also decreased upon treatment with the copolymeric particles P3HB/4HB10, <200 nm. Interestingly, size of P3HB particles did not alter the metabolic activity of these cells, being similar for both P3HB > 200 nm and P3HB < 200 nm particles ( $p \leq 0.05$ ), respectively. This phenomenon may be the consequence of the established marked hydrophobicity of P3HB.

Short-term cultivation of monocytes on P3BH and P3HB/4HB10 fibrous scaffolds was associated with discrete effects on viability. Indeed, only exposure to the P3HB substrates with oriented fibers caused noticeable decrease of optical density as compared to control, ( $p \leq 0.05$ ). Thus, it should be noted, that the orientation of fibers affects the ability of monocytes to reduce MTT. Indeed, in a recent report by Raman et al. (2016) it was shown that the morphology of NP and surface area determine their cytotoxicity, which may have implications for their biological application.

Cellular molecular mechanisms participating in MTT reduction are not fully established, and the participation of NAD(P)H-dependent oxidoreductases or other reducing molecules in electron transfer to the MTT are suggested (Marshall et al., 1995; Berridge et al., 2005). Indeed, it is indicated that the cellular reduction of MTT may depend on the activity of mitochondrial

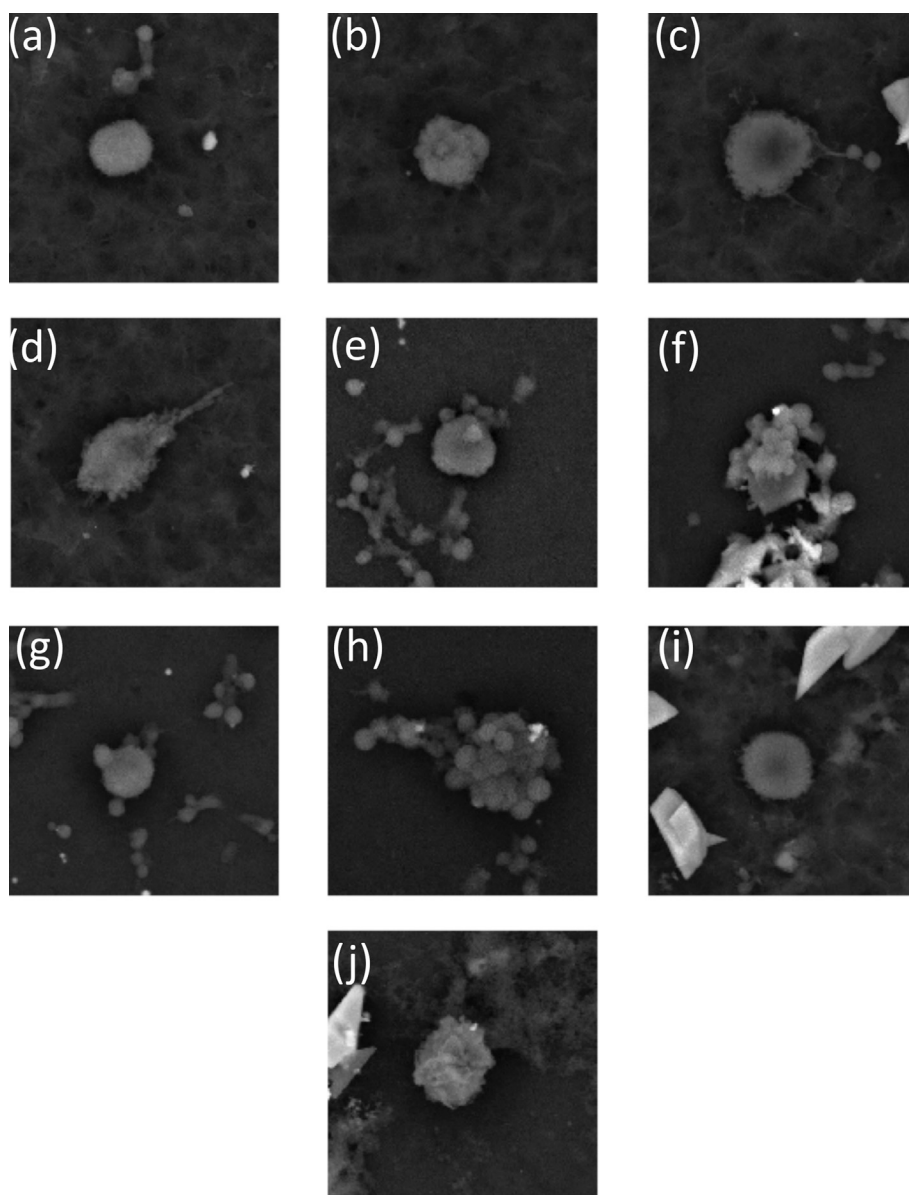


**Fig. 1.** Morphological types of monocytes in culture. Control morphological types (a, b, c, d): at the bottom of the 96-well culture plate sterile PHA-biopolymer scaffolds were placed and 104 cells in 160  $\mu$ L DMEM, 10% fetal serum per well were seeded. Cells were cultured for 36 h. Magnification  $\times$  4000. Treatment morphological types (e, f, g, h, i, j): monocytes were cultured in 96-well plates on sterile PHA-biopolymer scaffolds with various concentrations of fullerenes and nanodiamonds without a protein corona (F and ND, respectively); fullerenes and nanodiamonds with the protein corona (F + PC and ND + PC, respectively).  $10^4$  cells in 80  $\mu$ L DMEM, 10% fetal serum and 80  $\mu$ L nanoparticle solutions in DMEM, 10% fetal serum were added to wells. Cells were cultured for 36 h. Magnification  $\times$  4000. a – spherical cell with “microvilli” on the surface (class 1 in Table 3); b – adherent cell with ruffles on the surface (the class 2 in Table 3); c – adherent “flat” cell with complicated membrane relief along the edge (class 3 in Table 3); d – macrophage like cell (class 4 in Table 3); e, f – treatment with F (25  $\mu$ g/mL), adherent “flat” cells with a smooth edge (class 5 in Table 3) in contact with single platelet (e), t group of aggregated platelets on the surface of the “flat” monocyte (f); g – treatment with F + PC (25  $\mu$ g/mL), spherical cell with “microvilli” on the surface (class 1 in Table 3) in contact with platelets; h – treatment with F (50  $\mu$ g/mL), macrophage-like monocyte is coated with platelets (class 6 in Table 3); i – treatment with ND (25  $\mu$ g/mL) and ND + PC (25  $\mu$ g/mL), adherent “flat” cell with complicated membrane relief along the edge (class 3 in Table 3). j – treatment with ND (50  $\mu$ g/mL), adherent cell with ruffles on the surface (class 2 in Table 3).

enzymes (Berridge and Tan, 1993; Berridge et al., 1996). Therefore, MTT reduction processes depend to a large extent, on the activity of metabolic cycles associated with NAD(P)H streams. Thus, cells with low metabolic activity, as thymocytes and splenocytes, reduce lower amounts of MTT. It must be pointed out that under certain culture conditions the changes in metabolic activity can be responsible for the changes in metabolic activity are responsible for lower cellular reduction of MTT and not the decrease in cell viability (Berridge and Tan, 1993, 1996; Safi et al., 2016). Our results indicate a high “sensitivity” of monocyte culture test system for the integrated evaluation of the biological activities of BNMs with different composition, dimensions and morphological features.

### 3.2. Effect of F and ND on MTT reduction activity and morphology of monocytes

In continuation we evaluated the effects of F and ND particle treatment on monocyte viability. In some experiments, in order to perform comparative assessment, these particles were functionalized with a protein “corona”. In treatments with F-particles no affect on monocyte viability was evident as compared to the control (cultivation on P3HB/4HB10 film scaffolds) at all studied concentrations (Table 2). Pre-coating of F with a protein corona, F + PC, had no further effect. Interestingly, when monocytes were treated with ND in concentrations up to 50  $\mu$ g/mL, the cellular reduction of MTT

**Table 3**  
The effects of NPs treatments on monocyte morphology.

Treatment types	Morphological classes of monocytes					
	1. Spherical cells with “microvilli” on the surface	2. Adherent cells with ruffles on the surface	3. Adherent “flat” cells with complicated membrane relief along the edge	4. Macrophage like cells	5. Adherent “flat” cells with a smooth edge	6. Macrophage like cells, “covered” by platelets
P3HB/4HB10 <sup>b</sup> (control)	54 ± 6,5 <sup>a</sup>	21 ± 3,2	11 ± 1,3	14 ± 1,8	0	0
P3HB/4HB10 + F, 25 µg/mL	8 ± 1,1	4 ± 0,6	4 ± 0,7	4 ± 0,5	80 ± 10,3	0
P3HB/4HB10 + (F + PC), 25 µg/mL	50 ± 6,7	33 ± 4,2	17 ± 2,1	0	0	0
P3HB/4HB10 + F, 50 µg/mL	24 ± 2,5	1 ± 0,3	10 ± 1,4	13 ± 1,7	0	50 ± 4,5
P3HB/4HB10 + ND, 25 µg/mL	55 ± 6,2	10 ± 1,4	20 ± 2,4	5 ± 0,8	10 ± 1,3	0
P3HB/4HB10 + (ND + PC), 25 µg/mL	40 ± 4,8	13 ± 1,6	47 ± 5,2	0	0	0
P3HB/4HB10 + ND, 50 µg/mL	50 ± 5,6	43 ± 5,1	2 ± 0,3	5 ± 0,7	0	0
P3HB/4HB10 + (ND + PC), 50 µg/mL	70 ± 8,1	11 ± 1,5	15 ± 1,8	4 ± 0,6	0	0

<sup>a</sup> The results are expressed as % of total number of analyzed cells.

<sup>b</sup> The thickness of film scaffolds was 115 ± 16 µm, with an average diameter of 6 mm, well in correlation to the diameter the 96-well plate.

was increased (Table 2). This may be due to enhanced production of reactive oxygen species in the mitochondria compartment of monocytes (Garn et al., 1994). F and ND exhibit differences in size and structure, as is described in Materials and Methods section, and, respectively, in the composition/structure of proteins in their PCs, which may justify the differences in their biological activity. However, in treatments with NDs bearing PC, at the concentration of 50 µg/mL, the MTT cellular reduction was even lower as compared to the controls. These data suggests that the protein corona may enhance both the internalization of ND and ND-dependent intracellular effects, in particular the pool of reducing agents, involved in the reactions with MTT.

The processes of F and NDs internalization and subsequent reactions involving intracellular signaling pathways can be accompanied by significant restructuring of the plasma membrane and cell morphology as a whole. Therefore, the next stage of our study was to perform the morphological analysis of cells under various culture conditions.

### 3.3. The effects of NPs on monocyte morphology

Electron microscopy demonstrated that NPs have a type and structure –dependent effect on monocyte phenotype (Fig. 1, Table 3). Under the control conditions, e.g. culture on P3HB/4HB10 substrates, four monocyte phenotypes were evident; the dominant being spherical cells with “microvilli” on the surface (54% of the total cell population) (class 1 in Table 3, Fig. 1a). In addition, adherent cells with ruffles on the surface, (21%) (class 2 in Table 3, Fig. 1b), adherent “flat” cells with complicated membrane bas-relief along the edge, (11%) (class 3 in Table 3, Fig. 1c) and macrophage like cells, 14% (class 4 in Table 3, Fig. 1d) were observed.

The morphological heterogeneity of adherent monocytes *in vitro* could be attributed to the existence of various morpho-functional subpopulations of circulating monocytes in the bloodstream (Stansfield and Ingram, 2015; Mikołajczyk et al., 2016). After the isolation from blood, subpopulations of monocytes implement specific differentiation programs in culture *in vitro*, particularly as regarding reorganization of the cytoplasmic membrane and the

supporting cytoskeleton structure (Di Cosmo-Ponticello et al., 2014; Brown et al., 2014). As a result, the heterogeneity of the cell population is maintained under *in vitro* conditions (Safi et al., 2016).

Exposure to different NPs results in significant changes as regarding the ratio among respective phenotypes of monocytes (Table 3). Moreover, exposure in the case of F particles at a concentration 25 µg/mL led to the appearance of a new morphological class of cells – adherent “flat” cells with a smooth edge (class 5 in Table 3, Fig. 1e, f). Cells of this type were often observed in contact with platelets. However, when F particles at (25 µg/mL), were coated with a PC the phenotype of adherent “flat” cells with a smooth edge was not detected, whereas the dominant phenotype was that of spherical cells with “microvilli” on the surface (class 1 in Table 3, Fig. 1g). Interestingly, exposure to F (50 µg/mL) resulted in the appearance of a new morphological class – macrophage like cells, whose surface was “covered” by platelets (class 6 in Table 3, Fig. 1h). Exposure to ND induced different quantitative relationships between phenotypes, discrepant from both - the control and treatment with F (Table 3). Moreover, the effects of ND with PC were significantly different from the effects of ND without it (“naked” ND). Thus, the number of “flat” cells with complicated membrane edge (class 3 in Table, Fig. 1i) was 2 times higher for ND with the protein “corona” as compared for “naked” ND (concentration 25 µg/mL). Based on these results we can assume that the interaction in direct contact of F and ND with different subpopulations of peripheral blood monocytes leads to significant changes in the processes of morphological differentiation of these cell subpopulations *in vitro*. Indeed, this may reflect the functional monocyte-macrophage activity *in vitro* as regarding the ratio of phenotypes M1 and M2, which may vary substantially among different donors (Damanik et al., 2014; Grotenhuis et al., 2014). The exposure of monocytes to NPs, currently in use as a biocompatible implantable materials for medical purposes, exhibited discrete effects on their morphology depending on their chemical structure and utilized processing techniques (Lu & Webster, 2015). Thus, under the influence of F the subpopulation of monocytes differentiated, exhibiting increased adhesiveness for platelets. This phenomenon could be a putative consequence of the activation of

cytokines synthesis, which attract platelets, as well as of alterations in the expression of specific adhesion molecules which contribute to platelet-monocyte adhesion patterns. It should also be noted, that in the contact groups-monocyte-platelets, the last maintained a smooth spherical shape.

In the present study the interaction of NPs was evaluated at two levels: (i) internalization of NPs and (ii) interaction of monocytes with biopolymeric scaffolds. During these interactions adhesive contacts were formed between cells and NPs where cells exert mechanical force. This idea comes from studies of adhesive properties of cells where specific adhesion molecules, e.g. integrins act as mechanical conduits between the extracellular matrix and the cytoskeleton located to cell interior (Klotzsch et al., 2015). The generated mechanical forces have the ability to rearrange proteins laterally, which may result in protein clustering as well as regulate their specific activities (Gomez and Billadeau, 2008).

In other model systems the incorporation of natural products, including heparin and its derivatives leads to morphological changes in the actin cytoskeleton and altered melanoma adhesion and migration properties. Thus, heparin uptake inhibits melanoma cell adhesion and migration (Chalkiadaki et al., 2011a,b). In our experimental model the specific interactions with discrete NPs are translated in morphological changes of monocytes.

In summary, effects of F and ND on the processes of morphological and functional differentiation of monocyte subpopulations can be realized: a) through the system of receptor-dependent internalization; b) through non-receptor interactions of NPs with the plasma membrane and the activation of mechano-chemical signaling. Further studies are necessary to determine the contribution of the proposed approaches. The demonstrated marked changes of monocyte phenotypes during exposure to NPs, under short-term cultivation, allow the use of morphological criteria for preliminary assessment of effects that various structural types of biopolymeric nanomaterials exert.

#### 4. Conclusion

In conclusion, the ability of monocytes to reduce MTT upon exposure to BMPs of particular or fibrous morphology, under short term culture, is dependent on BNMs-chemical composition, size and morphological characteristics. The effects were dependent on fiber orientation and concentration of particles in suspensions as well as on the existence of a protein corona. Short-term culture of monocytes is a potentially suitable model system for the evaluation of nanomaterials' biological effects. Further, research is needed in order to develop and validate these tests for the purpose of efficient BNP assessment.

#### Conflict of interest

No conflict of interest to declare.

#### Transparency document

Transparency document related to this article can be found online at <http://dx.doi.org/10.1016/j.fct.2016.08.025>.

#### References

Anderson, J.M., 2015 Mar. Exploiting the inflammatory response on biomaterials research and development. *J. Mater. Sci. Mater. Med.* 26 (3), 121. <http://dx.doi.org/10.1007/s10856-015-5423-5>. Epub 2015 Feb 18.

Berridge, M.V., Tan, A.S., 1993. Characterization of the cellular reduction of 3-(4,5-dimethylthiazol-2-yl)-2,5-diphenyltetrazolium bromide (MTT): subcellular localization, substrate dependence, and involvement of mitochondrial electron transport in MTT reduction. *Arch. Biochem. Biophys.* 303, 474–482.

Berridge, M., Tan, A., McCoy, K., Wang, R., 1996. The biochemical and cellular basis of cell proliferation assays that use tetrazolium salts. *Biochemica* 4, 14–19.

Berridge, M.V., Herst, P.M., Tan, A.S., 2005. Tetrazolium dyes as tools in cell biology: new insights into their cellular reduction. *Biotechnol. Annu. Rev.* 11, 127–152.

Bharde, A.A., Palankar, R., Fritsch, C., Klaver, A., Kanger, J.S., Jovin, T.M., Arndt-Jovin, D.J., 2013. Magnetic nanoparticles as mediators of ligand-free activation of EGFR signaling. *PLoS One* e68879. <http://dx.doi.org/10.1371/journal.pone.0068879>, 23;8(7).

Brown, S., Hutchinson, C.V., Aspinall-O'Dea, M., Whetton, A.D., Johnson, S.M., Rees-Unwin, K., Burtham, J., 2014. Monocyte-derived dendritic cells from chronic myeloid leukaemia have abnormal maturation and cytoskeletal function that is associated with defective localisation and signalling by normal ABL1 protein. *Eur. J. Haematol.* 93 (2), 96–102.

Chalkiadaki, G., Nikitovic, D., Katonis, P., Berdiaki, A., Tsatsakis, A., Kotsikogianni, I., Karamanos, N.K., Tzanakakis, G.N., 2011a. PKCa/JNK signaling pathway inducing actin cytoskeleton changes. *Cancer Lett.* 312 (2), 235–244.

Chalkiadaki, G., Nikitovic, D., Berdiaki, A., Katonis, P., Karamanos, N.K., Tzanakakis, G.N., 2011b. Heparin plays a key regulatory role via a p53/FAK-dependent signaling in melanoma cell adhesion and migration. *IUBMB Life* 63 (2), 109–119.

Curtis, A.S., Tsimbouri, P.M., 2014. Epigenesis: roles of nanotopography, nanoforces and nanovibration. *Expert Rev. Med. Devices* 11 (4), 417–423.

Damanik, F.F.R., Rothuizen, T.C., van Blitterswijk, C., Rotmans, J.L., Moroni, L., 2014. Towards an in vitro model mimicking the foreign body response: tailoring the surface properties of biomaterials to modulate extracellular matrix. *Sci. Rep.* 4, 6325. <http://dx.doi.org/10.1038/srep06325>.

Di Cosmo-Ponticello, C.J., Hoover, D., Coffman, F.D., Cohen, S., Cohen, M.C., 2014. MIF inhibits myocytic movement through a non-canonical receptor and disruption of temporal Rho GTPase activities in U-937 cells. *Cytokine* 69 (1), 47–55.

Di Silvio, D., Rigby, N., Bajka, B., Mackie, A., Baldelli Bombelli, F., 2015. Effect of protein corona magnetite nanoparticles derived from bread in vitro digestion on Caco-2 cells morphology and uptake. *Int. J. Biochem. Cell Biol.* 75, 212–222.

Echarri, A., Del Pozo, M.A., 2015. Caveolae - mechanosensitive membrane invaginations linked to actin filaments. *J. Cell Sci.* 128 (15), 2747–2758.

Farokhzad, O.C., Langer, R., 2006. Nanomedicine: developing smarter therapeutic and diagnostic modalities. *Adv. Drug Deliv. Rev.* 58 (14), 1456–1459.

Fleischer, C.C., Payne, C.K., 2014. Nanoparticle-cell interactions: molecular structure of the protein corona and cellular outcomes. *Acc. Chem. Res.* 47 (8), 2651–2659.

Galic, M., Begemann, I., Viplav, A., Matis, M., 2014. Force-control at cellular membranes. *Bioarchitecture* 4 (4–5), 164–168.

Garn, H., Heidi, K., Volker, E., 1994. An improved MTT assay using the electron-coupling agent menadione. *J. Immunol. Methods* 168, 253–256.

Gomez, T.S., Billadeau, D.D., 2008. T cell activation and the cytoskeleton: you can't have one without the other. *Adv. Immunol.* 97, 1–64.

Grotenhuis, N., Vd Toom, H.F., Kops, N., Bayon, Y., Deerenberg, E.B., Mulder, I.M., van Osch, G.J., Lange, J.F., Bastiaansen-Jenniskens, Y.M., 2014 Jul. In vitro model to study the biomaterial-dependent reaction of macrophages in an inflammatory environment. *Br. J. Surg.* 101 (8), 983–992. <http://dx.doi.org/10.1002/bjs.9523>.

Hata, K., Higashisaka, K., Nagano, K., Mukai, Y., Kamada, H., Tsunoda, S., Yoshioka, Y., Tsutsumi, Y., 2014. Evaluation of silica nanoparticle binding to major human blood proteins. *Nanoscale Res. Lett.* 9 (1), 2493.

Henstock, J., Haj, A., 2015. Controlled mechanotransduction in therapeutic MSCs: can remotely controlled magnetic nanoparticles regenerate bones. *Regen. Med.* 10 (4), 377–380.

Henstock, J.R., Rotherham, M., Rashidi, H., Shakesheff, K.M., El Haj, A.J., 2014. Remotely activated mechanotransduction via magnetic nanoparticles promotes mineralization synergistically with bone morphogenetic protein 2: applications for injectable cell therapy. *Stem Cells Transl. Med.* 3 (11), 1363–1374.

Khalili, F.J., Jafari, S., Eghbal, M.A., 2015. A Review of molecular mechanisms involved in toxicity of nanoparticles. *Adv. Pharm. Bull.* 5 (4), 447–454.

Kilinc, D., Dennis, C.L., Lee, G.U., 2016. Bio-nano-magnetic materials for localized mechanochemical stimulation of cell growth and death. *Adv. Mater.* 28, 5672–5680. <http://dx.doi.org/10.1002/adma.201504845>.

Klotzsch, E., Stiegler, J., Ben-Ishay, E., Gaus, K., 2015. Do mechanical forces contribute to nanoscale membrane organisation in T cells? *Biochim. Biophys. Acta* 1853 (4), 822–829.

Kuskov, A., Voskresenskaya, A.A., Goryachaya, A.V., Shtilman, M.I., Spandidos, D.A., Rizos, A.K., Tsatsakis, A.M., 2010. Amphiphilic poly-N-vinylpyrrolidone nanoparticles as carriers for non-steroidal anti-inflammatory drugs: characterization and in vitro controlled release of indomethacin. *Int. J. Mol. Med.* 26 (1), 85–94.

Lee, J.H., Kim, J.W., Levy, M., Kao, A., Noh, S.H., Bozovic, D., Cheon, J., 2014. Magnetic nanoparticles for ultrafast mechanical control of inner ear hair cells. *Am. Chem. Soc. Nano* 8 (7), 6590–6598.

Lu, J., Webster, T.J., 2015 Apr. Reduced immune cell responses on nano and sub-micron rough titanium. *Acta Biomater.* 16, 223–231. <http://dx.doi.org/10.1016/j.actbio.2015.01.036>.

Marshall, N.J., Goodwin, C.J., Holt, S.J., 1995. A critical assessment of the use of microculture tetrazolium assays to measure cell growth and function. *Growth Regul.* 5 (2), 69–84.

Majd, H., Scherer, S.S., Boo, S., Ramondetti, S., Cambridge, E., Raffoul, W., Friedrich, M., Pittet, B., Pioletti, D., Hinz, B., Pietramaggiore, G., 2015 Jun. Novel micropatterns mechanically control fibrotic reactions at the surface of silicone implants. *Biomaterials* 54, 136–147. <http://dx.doi.org/10.1016/j.biomaterials.2015.03.027>.

Matczuk, M., Anecka, K., Scaletti, F., Messori, L., Keppler, B.K., Timerbaev, A.R.,

- Jarosz, M., 2015. Speciation of metal-based nanomaterials in human serum characterized by capillary electrophoresis coupled to ICP-MS: a case study of gold nanoparticles. *Metalomics* 7 (9), 1364–1370.
- Mikołajczyk, T.P., Osmenda, G., Batko, B., Wilk, G., Krezelok, M., Skiba, D., Sliwa, T., Pryjma, J.R., Guzik, T.J., 2016. Heterogeneity of peripheral blood monocytes, endothelial dysfunction and subclinical atherosclerosis in patients with systemic lupus erythematosus. *Lupus* 25 (1), 18–27.
- Mortimer, G.M., Butcher, N.J., Musumeci, A.W., Deng, Z.J., Martin, D.J., Minchin, R.F., 2014. Cryptic epitopes of albumin determine mononuclear phagocyte system clearance of nanomaterials. *Am. Chem. Soc. Nano* 8 (4), 3357–3366.
- Neagu, M., Piperigkou, Z., Karamanou, K., Engin, A.B., Docea, A.O., Constantin, C., Negrei, C., Nikitovic, D., Tsatsakis, A., 2016. Protein bio-corona: critical issue in immune nanotoxicology. *Arch. Toxicol.* 1–18. <http://dx.doi.org/10.1007/s00204-016-1797-5>.
- Parameswaran, S., Verma, R.S., 2011. Scanning electron microscopy preparation protocol for differentiated stem cells. *Anal. Biochem.* 416 (2), 186–190.
- Piperigkou, Z., Karamanou, K., Engin, A.B., Gialeli, C., Docea, A.O., Vynios, D.H., Pavão, M.S., Golokhvast, K.S., Shtilman, M.I., Argiris, A., Shishatskaya, E., Tsatsakis, A.M., 2016. Emerging aspects of nanotoxicology in health and disease: from agriculture and food sector to cancer therapeutics. *Food Chem. Toxicol.* 91, 42–57.
- Polyak, B., Cordovez, B., 2016. How can we predict behavior of nanoparticles in vivo. *Nanomed. Lond.* 11, 189–192. <http://dx.doi.org/10.2217/nnm.15.192>.
- Raman, V., Suresh, S., Savarimuthu, P.A., Raman, T., Tsatsakis, A.M., Golokhvast, K.S., Vadivel, V.K., 2016. Synthesis of Co3O4 nanoparticles with block and sphere morphology, and investigation into the influence of morphology on biological toxicity. *Exp. Ther. Med.* 11, 553–560.
- Recalde, H.R., 1984. A simple method of obtaining monocytes in suspension. *J. Immunol. Methods* 69 (1), 71–77.
- Safi, W., Kuehnl, A., Nüssler, A., Eckstein, H.H., Pelisek, J., 2016. Differentiation of human CD14+ monocytes: an experimental investigation of the optimal culture medium and evidence of a lack of differentiation along the endothelial line. *Exp. Mol. Med.* 48, e227. <http://dx.doi.org/10.1038/emm.2016.11>.
- Shannahan, J.H., Podila, R., Brown, J.M., 2015. A hyperspectral and toxicological analysis of protein corona impact on silver nanoparticle properties, intracellular modifications, and macrophage activation. *Int. J. Nanomed.* 10, 6509–6521.
- Shishatskaya, E.I., Nikolaeva, E.D., Goreva, A.V., Brigham, C.J., Volova, T.G., Sinskey, A.J., 2012. Investigation in vivo of films made of resorbable polyhydroxyalkanoates with different composition: tissue reaction and kinetics of biodestruction. *Cell Transplant. Tissue Eng.* 7, 73–80 (In Russian).
- Stansfield, B.K., Ingram, D.A., 2015. Clinical significance of monocyte heterogeneity. *Clin. Transl. Med.* 4, 5. <http://dx.doi.org/10.1186/s40169-014-0040-3>.
- Trindade, R., Albrektsson, T., Tengvall, P., Wennerberg, A., 2016 Feb. Foreign body reaction to biomaterials: on mechanisms for buildup and breakdown of osseointegration. *Clin. Implant. Dent. Relat. Res.* 18 (1), 192–203.
- Zandstra, J., Hiemstra, C., Petersen, A.H., Zuidema, J., van Beuge, M.M., Rodriguez, S., Lathuile, A.A., Veldhuis, G.J., Steendam, R., Bank, R.A., Poppa, E.R., 2014 Oct 28. Microsphere size influences the foreign body reaction. *Eur. Cell Mater* 28, 335–347.
- Zanganeh, S., Spitler, R., Erfanzadeh, M., Mahmoudi, M., 2016. Protein corona: opportunities and challenges. *Int. J. Biochem. Cell Biol.* 75, 143–147.